PCCP

Accepted Manuscript

ROYAL SOCIETY OF CHEMISTRY

www.rsc.org/pccp

Cite this: DOI: 10.1039/c0xx00000x

www.rsc.org/xxxxxx

PAPER

Fabrication of hydrogel-coated single conical nanochannels exhibiting controllable ion rectification characteristics†

Linlin Wang,[a] Huacheng Zhang,*[b] Zhe Yang,[a] Jianjun Zhou,*[a] Liping Wen,[c] Lin Li[a] and Lei Jiang[b,c]

Received (in XXX, XXX) Xth XXXXXXXXX 20XX, Accepted Xth XXXXXXXXX 20XX

DOI: 10.1039/b000000x

Heterogeneous nanochannel materials that endow new functionalities different to the intrinsic properties of two original nanoporous materials have wide potential applications in nanofluidics, energy conversion, and biosensors. Herein, we report novel interesting hydrogel-composited nanochannel devices with regulatable ion rectification characteristics. The heterogeneous nanochannel devices were constructed by selectively coating the tip side, base side, and both sides of a single conical nanochannel membrane with thin agar hydrogel layers. Tunable ion current rectifications of the nanochannel under the three different coating states were systematically demonstrated by current–voltage (*I*–*V*) curves. The asymmetric ionic transport property of the conical nanochannel was further strengthened in the tip-coating state and weakened in the base-coating state, respectively, whereas the conical nanochannel showed nearly symmetric ionic transport in the dual-coating state. Repeated experiments presented a better insight into the good stability and reversibility of the three coating states of the hydrogel-nanochannel-integrated systems. This work, as an example, may provide a new strategy to further design and develop multifunctional gel-nanochannel heterogeneous smart porous nanomaterials.

1. Introduction

Ion channels that intelligently control over transport of diverse ions through cell membranes are essential for life activities.[1] Ion rectification which ions flow in a preferential direction is one vital characteristic of biological ion channels.[1-3] Inspired by biological ion channels, creation of artificial nanochannels with smart functionalities in terms of controllable ionic transport has attracted extensive research interests.[4-13] Generally, artificial single nanochannels can be endowed with ion rectification characteristics by rationally designing an asymmetric charge distribution inside the nanochannel.[4, 14-18] There has been rapid progress in developing asymmetrically charged artificial single nanochannels that could strongly rectify ion current via asymmetric design of the channel shapes[19-24] and asymmetric modification of the inner surfaces of the channels with different responsive molecules.[25-29] In addition to the asymmetric surface charge distribution, wettability on the channel surface is another important factor to regulate ion transport of the nanochannel.[8, 30-32] And theoretical modelling has confirmed that a nanochannel with asymmetric wettability on the surface is beneficial to unidirectional water and ion transport.[33] However, little attention has been paid to fabrication of the synthetic nanofluidic device with non-homogeneous wettability.

Recently, heterogeneous nanochannel materials have attracted increasing interests because they may endow new functions different to the intrinsic properties of two original nanochannel materials, which play important roles in nanofluidic diodes and energy conversions.[34-36] The most representative case among heterogeneous nanochannel materials is the ionic diode, which allows unidirectional ion transport by a couple of the negatively charged mesoporous-carbon membrane and positively charged macroporous-alumina film.[34] Therefore, it is of great significance to create easily available heterogeneous nanochannel materials based on two nanochannel membranes with different wettabilities and surface charges.

In this work, we further demonstrate novel heterogeneous nanofluidic devices with both non-homogeneous wettability and asymmetric surface charge distribution exhibiting tunable ionic transport properties. The heterogeneous nanodevice comprises of a super-hydrophilic agar hydrogel layer and a hydrophilic single conical nanochannel membrane, and demonstrates its privilege in tuning the ion rectification characteristics by its non-uniform interfacial wettability and charge density. In addition, the nanochannel can still be restored to its original characteristics after removing the coated agar hydrogel. Such a composited nanochannel system could potentially spark further efforts with various functional hydrogels and different shaped single nanochannels to exploit more intelligent gel-nanochannel composited materials.

Here we select agar hydrogel as one original material to develop functional composited nanochannel materials because it is widespread in nature, and it could form supporting structure in cell walls.[37] Agar hydrogel has also been widely used for its advantages of non-toxic and highly compatibility in organisms,[38, 39] compared with other inorganic nanoporous membrane. Furthermore, negatively charged and super-hydrophilic natural agar gel[40, 41] has superior water retention and three-dimensional

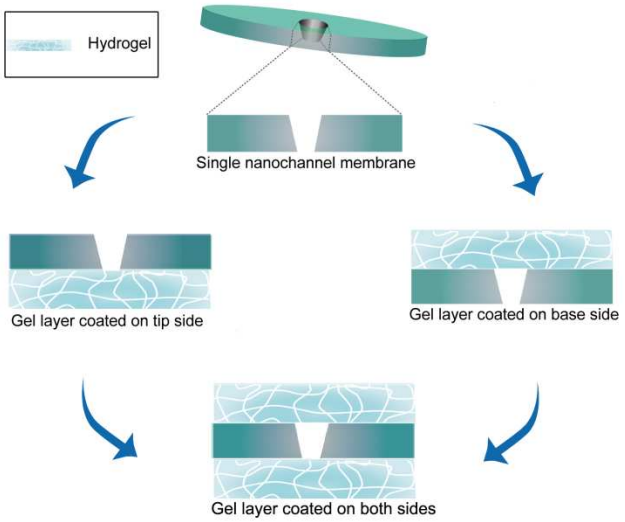

Scheme 1 Schematic demonstration of the single conical nanochannel composited with thin agar hydrogel layers. Tunable ion transport properties of the channel in stable external condition were observed after selective coating of the tip side, base side, and both sides of the nanochannel.

porous network structure.[42] In this case, we conduct our research to combine nanochannel with agar hydrogel to form a composite nanofluidic system. Thus, electrolyte solution can pass through the hydrogel under an electric field without significantly undertaking any extra resistance. In addition, considering the unique feature of agar gel that can be melt at high temperature, the agar gel layer could be easily removed from the nanochannel.[42, 43] And the original structure of nanochannel is well preserved after removing the agar gel. Besides, the stability of the agar hydrogel also guarantees its real application in vitro.

Scheme 1 illustrates the selective and reversible coating processes of a single conical nanochannel with thin agar hydrogel layers. The single nanochannel could be asymmetrically and symmetrically coated by the hydrogel film to form tip-, base- and dual-coating states of the gel-composed nanochannel. Tunable and reversible ion transport control of the gel-nanochannel device can be realized by alternating the nanochannel among the original and gel-composited states.

2. Experimental

Materials

Polyethylene terephthalate (PET) membranes (diameter of 3 cm, thickness of 12 μm, Hostaphan RN12 Hoechst) that had been irradiated with a heavy ion of 2.2 GeV kinetic energy to create a single damage track through the membrane were obtained from GSI, Darmstadt, Germany. Potassium chloride (KCl), sodium hydroxide (NaOH), performic acid (HCOOH), and agar powder used in the experiment were purchased from Beijing Chemical Reagent Company (Beijing, China). All of the chemicals were at least analytical grade. The water used throughout all experiments was purified by a Milli-Q system (Millipore, Bedford, MA, USA).

Nanochannel fabrication

The single conical nanochannels were produced in PET membranes by using the well-developed ion track etching technique.[19] To produce the conical nanochannels, the tracked membrane was etched by one side with etching solution (9 M NaOH) and the other side with the stopping solution (1 M KCl +1 M HCOOH) at 35℃. For observation of the etching process, the voltage (1 V) used to monitor the etching process was applied in such a way that the transmembrane ionic current can be observed as soon as the nanochannel opened. After about 35 min of etching, both sides of the membrane were changed to the stopping solution which is able to neutralize the etchant, thus slowing down and finally stopping the etching process. Obtained single conical nanochannels had a small tip side and a large base side. The geometric parameters and profiles of the conical nanochannels were observed by using scanning electron microscope (SEM, Hitachi S-4800, Japan) to characterize the multi-channel membranes (density of $10^8/cm^2$) etched under the same condition as the single conical nanochannels. The large base diameter (D) of the nanochannels could be directly measured by SEM, while the small tip diameter (d) was calculated by equation (1),[16, 44] where L is the length of the nanochannel, $k(c)$ is the specific conductivity of 1 M KCl solution, I is the ionic current of the cmulti-channel membrane, U is the applied voltage.

$$d = \frac{4LI}{\pi k(c)DU} \qquad (1)$$

Gel-nanochannel composited nanodevice construction

The agar hydrogel composited nanochannel devices were fabricated by coating one side or both sides of the single-nanochannel membrane with one or two thin agar hydrogel layers. Dissolved the agar powder into a transparent liquid at 100℃ then cooled to 50℃ at last. Pipetted 50 μL of the solution and dropped it onto the center of the single-nanochannel membrane. Then we pressed the agar droplet inside a 100 μm thick template, the droplet was spreaded on the membrane surface. After cooling about 15 min at room temperature, the spreaded solution became a 100 μm thick hydrogel layer on the surface of the nanochannel membrane. The thickness of the gel layer could be tuned by controlling of the volume of the agar solution and the thickness of the template. Moreover, because agar can be melt at high temperature (above 95 ℃), the coated gel layer could be removed from the nanochannel surface by using boiled water (100 ℃) to wash out the agar gel layer.[42, 43] After removing the gel layer, the single conical nanochannel could restore its original property. As a result, by reversibly coating and de-coating gel layers on the tip, base, and both sides of the conical nanochannel, three different gel-nanochannel composited nanofluidic device were constructed (Scheme 1). In contrast with previous works of heterogeneous nanochannel materials that the coated or deposited layers can't be removed once they have been coated or deposited on the nanoporous membrane surfaces, the reversible coating/de-coating feature of the agar hydrogel is essential for realizing the three different gel-nanochannel composited nanodevices based on one single conical nanochannel.

Current measurements

The ion transport properties of the nanofluidic devices were studied by measuring ionic currents through the conical nanochannels before and after coating of the agar hydrogel layers.

Ionic current was measured by a Keithley 6487 picoammeter (Keithley Instruments, Cleveland, OH). Each sample of the single-nanochannel PET membranes with or without the gel layers were mounted between two chambers of an electrochemical cell. Taking the tip-coated nanochannel for example, the experimental set up was shown in Fig. S1 (†ESI). Ag/AgCl electrodes were used to apply a transmembrane potential across the film. Forward voltage was the potential applied on the tip side of the nanochannel. The main transmembrane potential used in this work was a scanning voltage varied from –2 to +2 V with a 40 s period. The electrolyte in this work is 0.1 M KCl solution. In this work, each test was repeated 3 times to obtain the average current value at different applied voltages. The testing temperature was 25 °C.

3. Results and discussion

Fig. 1a shows the cross section of the wet gel-composited nanochannel membrane characterized by polarizing microscope (POM, Olympus-BX53, light source TH4-200). The gel-nanochannel composited membrane was further dried and studied by SEM (Fig. 1b). The thickness of the agar hydrogel layer was about 100 μm, and the gel film was porous in dry state (Fig. 1c). The base side of the nanochannel could be directly characterized by SEM at high magnification (Fig. 1d), and radii of the base sides of the conical nanochannels after etching 35 min ranged from ~465 nm to ~580 nm (Fig. S2, †ESI). The mean radius of the base side was 515 ± 24 nm. Average radius of the small tip side calculated from equation (1) was 42 ± 8 nm. In addition, SEM image of the cross sections of the conical nanochannel is well confirmed its conical shape (Fig. S3, †ESI).

To explore the un-uniform surface wettability of the gel-nanochannel heterogeneous film, the channel films before and after coating with the gel layers have been studied by contact angle (CA) measurements (Contact Angle Meter, OCA 20, Dataphysics company, Germany). The CA of the PET film surfaces before coating hydrogel layer (Fig. 2a) was larger than the one after coating (Fig. 2b). The results of the CA measurements showed that the coated gel layer could lead to a visible change of the surface wettability of the nanodevice from 54.1 ± 2.8° to 10.5 ± 0.7°. As a result, the gel composited nanochannel membrane has non-homogeneous surface wettability.

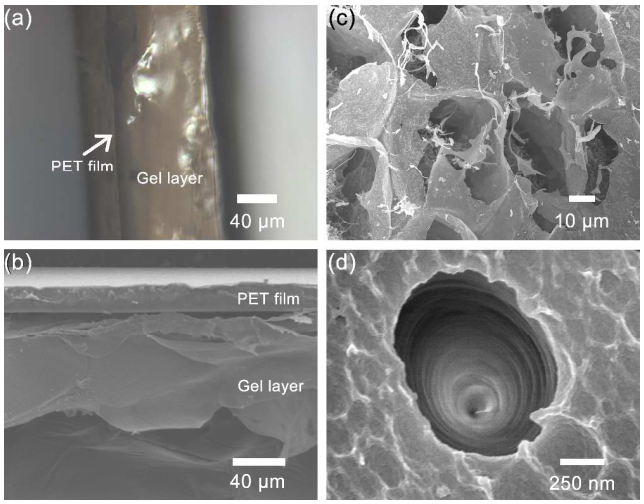

Fig. 1 (a) POM image of the agar hydrogel composited nanochannel in wet state. (b) SEM image of the hydrogel composited membrane in dry state. (c) Dried agar hydrogel network. (d) Base side of a conical nanochannel.

Ionic transport properties of the conical nanochannel (sample 1) before and after coating/de-coating the hydrogel layers were obtained by sequentially measuring the transmembrane ionic current of the channel at room temperature (25℃) in 0.1 M KCl solution. In the measuring procedure, the anode faced the tip side while the cathode faced the base side of the nanochannel. As shown in Fig. 3a, before coating, the initial conical nanochannel demonstrated the asymmetric *I–V* curve, indicating that the nanochannel has a preference in transporting ions from tip to base direction (Fig. 3a, black curve).[15, 45, 46] After coating the tip side of the nanochannel with a thin hydrogel layer, the nanochannel showed more asymmetric ion transport property (Fig. 3a, red curve). When de-coating the hydrogel on the tip side of the channel, the channel restored its original ionic transport property

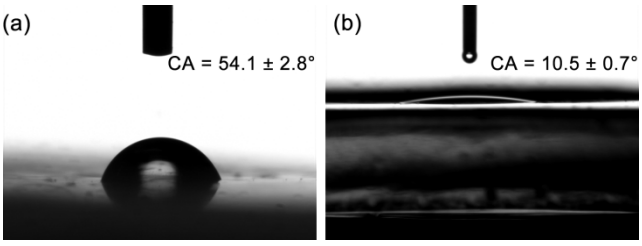

Fig. 2 The CA of the single-nanochannel PET film surfaces before and after coating an agar hydrogel layer. (a) Before coating. (b) After coating.

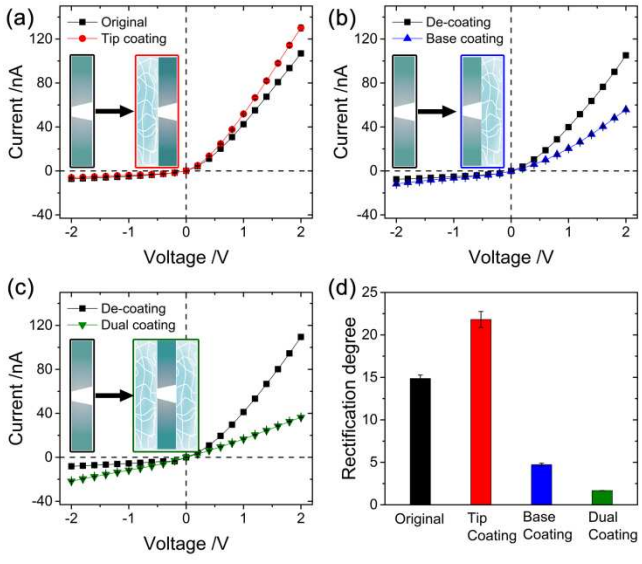

Fig. 3 *I–V* curves of a single nanochannel (sample 1) before and after composited with 100 μm agar hydrogel layers. (a) Original (■) and tip coating (●). (b) De-coating (■) and base coating (▲). (c) De-coating (■) and dual coating (▼). (d) Ion current rectification ratio of the original (black column), tip coating (red column), base coating (blue column) and dual coating (olive column) nanochannel.

(Fig. 3b, black curve). Whereas shifting the coating side to the base of the nanochannel, a considerable decrease of asymmetric *I–V* curve was observed (Fig. 3b, blue curve). The ionic current increased under negative voltage while dropped at positive voltage, where the variation was just the opposite of it in the tip side-coating sate. We further explored the ionic transport in the case of both-side coating after checking the original nanochannel property that was well preserved by de-coating the gel layer on the base side. As illustrated in Fig. 3c (olive curve), the *I–V* curve was almost symmetric, and it was quite different from the asymmetric ionic transports under tip and base coating states. As a result, without altering the external conditions, three different ionic transport properties were achieved in a conical nanochannel by selectively coating super-hydrophilic gel layers on the tip, base and both sides of the channel.

In order to quantify the influence of the hydrogel layer on ion current rectification (ICR) in this gel-composited nanochannel system, we define the ICR degree as the ratio of the current recorded at +2 V versus the absolute value of current recorded at –2 V. As shown in Fig. 3d, ICR ratio of the original nanochannel is 14.8 ± 0.4. When coating on the tip side of the channel, the ICR ratio increased to 21.8 ± 0.9 suggesting that the asymmetric ionic transport was enhanced by the gel layer. On the other hand, the ratio dropped substantially to 4.7 ± 0.2 but was still above 1 when coating on the base side, where the asymmetric ionic transport property was only weakened rather than just entirely disappeared. However, when both sides were coated with hydrogel, the ratio dropped to 1.67 ± 0.01 indicating that the nearly symmetric ionic transport property was achieved under this state. Hence, by controlling the asymmetric and symmetric coating, three diverse reversible ionic transport properties of the nanochannel were obtained in a stable external condition, which extends the limit of usually tuning the ionic transport of nanochannel with particular stimuli.

To obtain a better insight into the tunable ionic transport control in each coating case, we specifically considered the ionic current variation under the constant voltage –2 V and +2 V. Fig. 4 clearly showed the current gap of +2 V and –2 V in the original conical shaped nanochannel, where the asymmetric ionic transport was observed. When the tip side was first coated with agar hydrogel layer, ion current increased at +2 V while reduced at –2 V and the sign of the enlarged current gap was detected indicating that the asymmetric ionic transport was further strengthened. On the contrary, for coating on the base side, the current gap presented in the opposite trend, ion current reduced under +2 V while increased under –2 V. And in the both sides coating state, this tendency was further enhanced by observing the absolute value of ion currents were reaching almost the same.

Fig. 5 illustrates the proposed explanation of current rectification in the conical nanochannel before and after coating gel layer. Before coating, due to the presence of negatively charged carboxy groups on the channel wall, the asymmetrical geometry of the conical channel induces a preferential direction for cation transport from the tip to the base,[15, 16, 47] thus ion current of the conical nanochannel at positive voltage is much higher than that at negative voltage (Fig. 5a). After coating, because of the presence of negatively charged residues, such as sulfate, pyruvate and carboxy groups in natural agar,[41] the

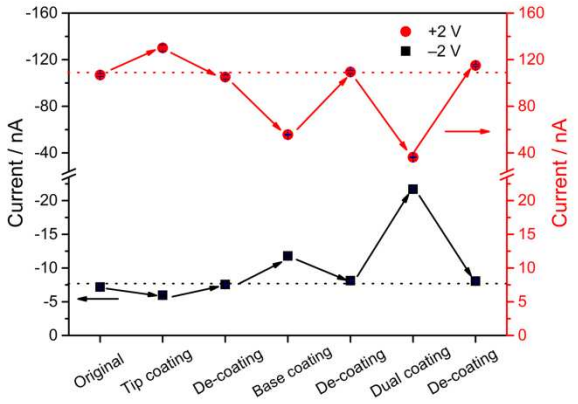

Fig. 4 The ion current variation of the nanochannel with the coating 100 μm agar hydrogel layer, and recovery after de-coating the gel layer at –2 V (black, ■) and +2 V (red, ●).

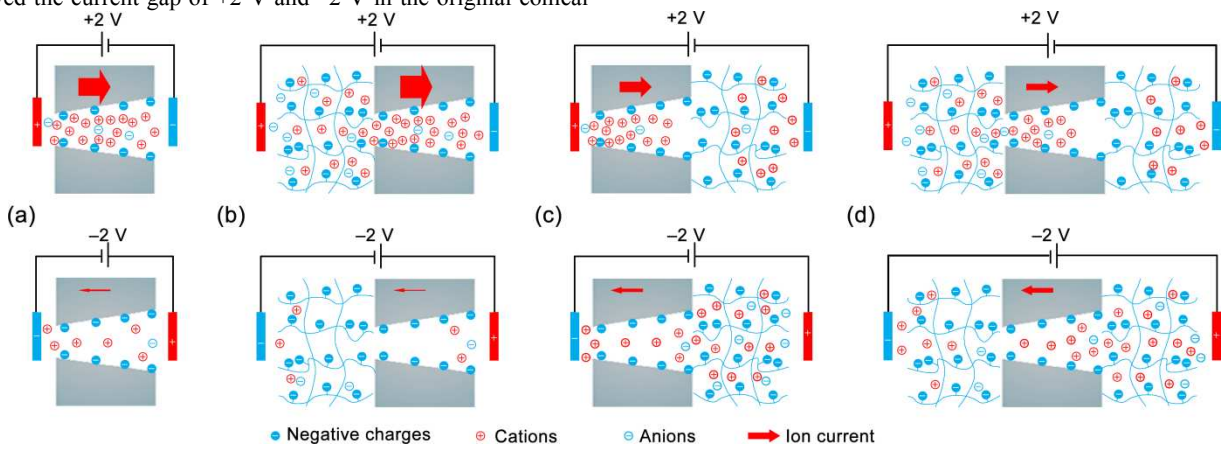

Fig. 5 Schematic illustration of the ion transport properties of the nanochannel before and after coating agar gel layer on the tip, base, and both sides at +2 V and –2 V. (a) The asymmetrical geometry of the conical channel induces a preferential direction for cation transport from the tip to the base. (b) For tip coating state, a forward electrochemical gradient induced by the negatively charged and super-hydrophilic gel layer (from tip to base) enhanced the degree of ICR. (c) For base coating state, a reversed electrochemical gradient (from base to tip) weaken the degree of ICR. (d) For dual coating state, two opposite electrochemical gradients nearly neutralized the ICR effect.

charged agar gel can also attract cations from the bulk solution into the gel layer, creating an electrochemical gradient from the coating side to non-coating side of the channel to impact ion transport through the channel (Fig. 5b-d). Under tip-coating state, the negatively charged and super-hydrophilic gel layer functions as an large electrical double layer at the tip side of the nanochannel can accelerate cations move into the nanochannel, while obstruct cations move out the nanochannel from the tip side. At positive applied voltage, ions rapidly accumulate into the gel layer and the nanochannel. The local concentrations become much higher than those in bulk solution, and a higher ion current is observed, compared with the current of the original nanochannel (Fig. 5b, up). When the polarity is switched to negative value, cations migrate outward from the gel layer and anions move out the channel from the base side, heading to the corresponding electrode, giving rise to a depleted zone in transition region between the channel and the gel layer, and consequently an increase of electric resistance caused by the lack of ions (Fig. 5b, down).[48-50] And obtained ion current is lower than the current of the original channel. However, under base-coating state, ion current reduces at positive voltage because the existing gel layer induces a depleted zone in transition region between the channel and the gel layer (Fig. 5c, up), while ion current increases at negative voltage because the negatiely charged gel layer makes cations easy to move into the nanochannel from the base side of the nanochannel compared with the un-coated channel (Fig. 5c, down). Under dual-coating state, ion currents at the positive and negative voltages become nearly equal because both positive and negative voltage can induce a depleted zone in transition region between the channel and the gel layer (Fig. 5d). Meanwhile, the two gel layers on the both sides of the nanochannel enhance the symmetry of the ion transport properties on the two directions of the dual-coating nanodevice by their same electric charge and super-hydrophilicity.

As well as its peculiar tunable ionic transport property, the composited nanochannel membrane also demonstrates good stability and reversibility. In order to eliminate the disturbance of cross experiments, we set out a series of repeated experiments by using three single conical nanochannels (samples 2–4) which have similar original ICR ratio, to conduct the tip coating, base coating and dual coating respectively. We repeated revisable "coating and de-coating" cycle in each single conical nanochannel for three times. As shown in Fig. 6, the tendency of *I–V* curves and ICR ratios variation in each coating case are consistent with the previous discussion. Besides, the ratios basically maintained stable in each "coating and de-coating" cycle. Therefore, the conical nanochannel can perfectly restore the original ratio after removing the coating layers and would again alter regularly according to the diverse coating states.

Furthermore, we have systematically investigated influences of the thickness of the gel layer, electrolyte concentration, and size of the nanochannel on the ion current rectification of the nanochannel before and after coating gel layer. First of all, a reproduced conical nanochannel sample 5 was used in this experiment. As shown in Fig. 7, although the ion current decreased with the increase of thickness of the gel layer, the ICR ratios of the channel after coating remained unchanged. This result indicated that increasing the thickness of gel layer is only equivalent to increase the resistance of the composited nanodevice, and the thickness of the gel layer didn't impact on the ion rectification characteristics of the nanodevices. Moreover, we systematically investigated ion transport properties of the gel-nanochannel devices based on different single conical nanochannels. As shown in Fig. S4 (†ESI), four original conical nanochannels performed similar *I–V* curves, and the four samples also had similar ion transport properties after coating agar hydrogel, which confirmed the reproducibility of the original conical nanochannels. Finally, ion current rectifications of a single conical nanochannel before and after tip, base, and dual coating under 0.01 M, 0.05 M, 0.1 M, 0.5 M and 1 M KCl solution have been measured. As shown in Fig. S5 (†ESI), although the rectification degrees are varied with changing ion concentrations, variations of the rectification degrees of the channel before and after coating under each test ion concentration are consistent. All experimental results proved that the functional ion transport could be easily available in a wide range of ion concentrations, nanochannels with different sizes, and differently thick gel layers.

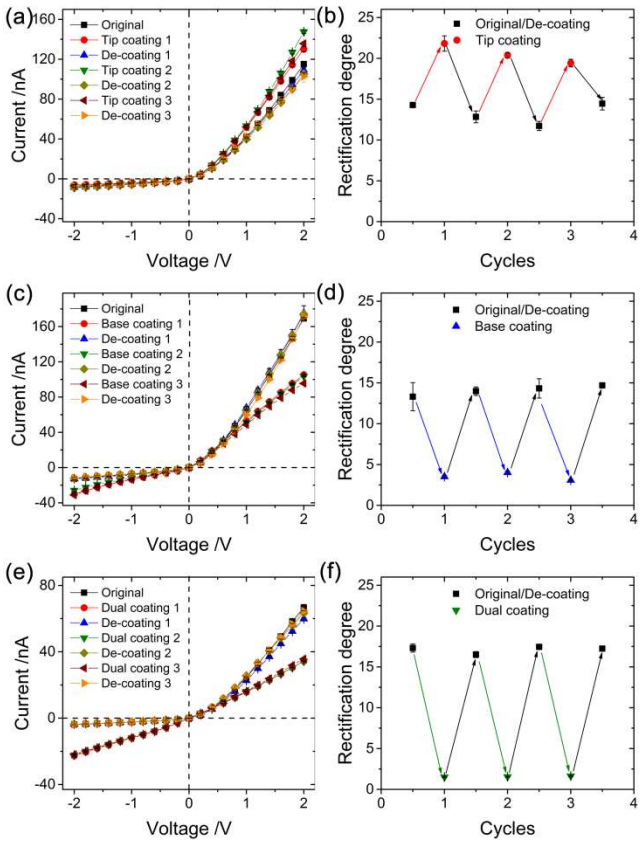

Fig. 6 Stability and reversibility of the 100 μm agar hydrogel layers composited nanochannel system were confirmed by repeating the "coating" and "de-coating" cycle for three times. (a,b) *I–V* curves and rectification ratios of the tip coating and de-coating cycles. (c,d) *I–V* curves and rectification ratios of the base coating and de-coating cycles. (e,f) *I–V* curves and rectification ratios of the dual coating and de-coating cycles. Experimental data were obtained from three conical nanochannels (samples 2 to 4) which have similar rectification ratios of the sample 1.

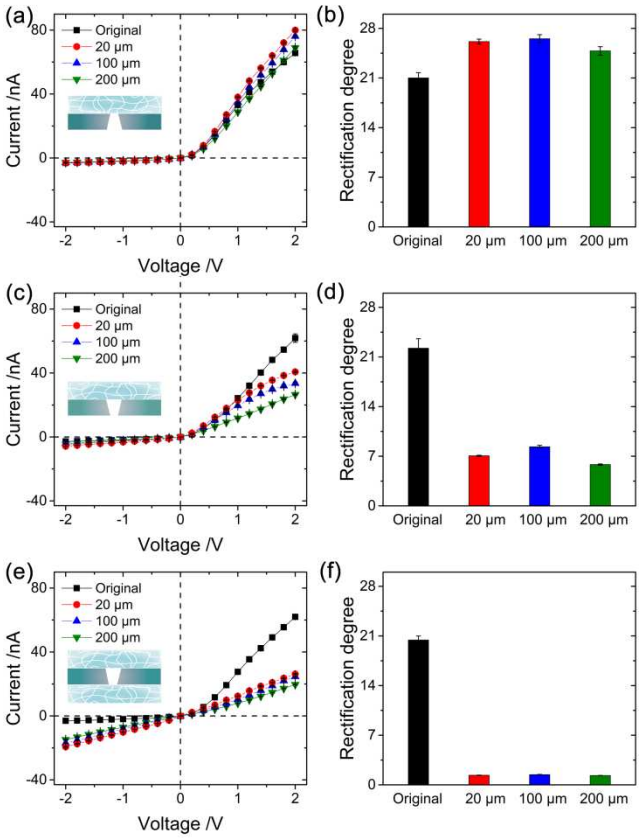

Fig. 7 *I–V* curves and rectification ratios of a single nanochannel (sample 5) before and after coating with different thick agar hydrogel layers (Original, ■, black; 20 μm, ●, olive; 100 μm, ▲, blue; 200 μm, red, ▼). (a,b) Tip coating; (c,d) Base coating; (e,f) Dual coating.

4. Conclusions

We have experimentally reported an agar hydrogel composited single conical nanochannel system with the enhanced functionality of tuning the ion rectification characteristic in a stable external condition by the surface charge and wettability differences between gel layer and nanochannel membrane. Through the selective coating of the tip, base, and both sides of the nanochannel, its asymmetric ionic transport was further strengthened, weakened, and even shift to symmetric ionic transport, respectively. Moreover, the ion transport property of the heterogeneous gel-nanochannel system was reversibly alternated among the three different coating sates. And the reversible gel coating method is suitable for different sized nanochannels to build functional composited nanofluidic devices. This work may potentially spark further experimental and theoretical efforts to fabricate more functional hydrogel-nanochannel heterogeneous materials in vitro and boost the development of applicable intelligent and flexible nanochannel apparatus for unidirectional water and ion transport, seawater desalination, and energy conversion.

Acknowlegements

The authors would like to give thanks to the Material Science Group of GSI (Darmstadt, Germany) for providing the ion-irradiated samples. This work was supported by the National Research Fund for Fundamental Key Projects (2011CB935700), National Science and Technology Major Project of the Ministry of Science and Technology of China (2013ZX09J13110-11B), The national science foundation of China: 21434003, the fundamental research funds for the central universities, and Beijing Key Laboratory of Energy Conversion and Storage Materials.

Notes and references

[a] *Beijing Key Laboratory of Energy Conversion and Storage Materials College of Chemistry, Beijing Normal University, Beijing, China. Fax: +86-010-6220-6152;Tel:+86-010-6220-6152; E-mail: pla_zjj@ bnu. edu.cn*

[b] *Laboratory of Bio-inspired Smart Interfacial Science, Technical Institute of Physics and Chemistry, Chinese Academy of Sciences, Beijing 100190，P. R. China. Fax:+86-010-8268-7566;Tel:+86-010-8254-3510;E-mail:zhanghc@mail.ipc.ac.cn*

[c] *Beijing National Laboratory for Molecular Sciences, Key Laboratory of Organic Solids, Institute of Chemistry, Chinese Academy of Sciences, Beijing, 100190,P. R. China. Fax:+86-010-8268-7566;Tel:+86-010-8262-1396*

† Electronic Supplementary Information (ESI) available: SEM images of the cross sections of the conical nanochannel film, contact angle of the gel layer and nanochannel surface, *I–V* curves and rectification ratios of four different sized conical nanochannels before and after coating with agar hydrogel layers. See DOI: 10.1039/b000000x/

1 B. Hille, *Ion Channels of Excitable Membranes*, Sinauer Associates, Massachusetts, Sunderland, MA, 2001.
2 N. Inagaki, *Science*, 1995, **270**, 1166.
3 C. A. Vandenberg, *Proc. Natl. Acad. Sci.*, 1987, **84**, 2560.
4 L. J. Cheng and L. J. Guo, *Chem. Soc. Rev.*, 2010, **39**, 923.
5 B. N. Miles, A. P. Ivanov, K. A. Wilson, F. Dogan, D. Japrung and J. B. Edel, *Chem. Soc. Rev.*, 2013, **42**, 15.
6 Z. S. Siwy and S. Howorka, *Chem. Soc. Rev.*, 2010, **39**, 1115.
7 M. Ali, P. Ramirez, S. Nasir, Q.-H. Nguyen, W. Ensinger and S. Mafe, *Nanoscale*, 2014, **6**, 10740.
8 M. Ali, P. Ramirez, M. N. Tahir, S. Mafe, Z. Siwy, R. Neumann, W. Tremel and W. Ensinger, *Nanoscale*, 2011, **3**, 1894.
9 L. Wang, Y. Yan, Y. Xie, L. Chen, J. Xue, S. Yan and Y. Wang, *Phys. Chem. Chem. Phys.*, 2011, **13**, 576.
10 M. Ali, P. Ramirez, H. Q. Nguyen, S. Nasir, J. Cervera, S. Mafe and W. Ensinger, *ACS Nano*, 2012, **6**, 3631.
11 D. G. Haywood, A. Saha-Shah, L. A. Baker and S. C. Jacobson, *Anal. Chem.*, 2014, DOI: 10.1021/ac504180h.
12 B. V. V. S. P. Kumar, K. V. Rao, S. Sampath, S. J. George and M. Eswaramoorthy, *Angew. Chem. Int. Ed.*, 2014, DOI: 10.1002/anie.201406448.
13 Y. Choi, L. A. Baker, H. Hillebrenner and C. R. Martin, *Phys. Chem. Chem. Phys.*, 2006, **8**, 4976.
14 P. Y. Apel, I. V. Blonskaya, O. L. Orelovitch, P. Ramirez and B. A. Sartowska, *Nanotechnology*, 2011, **22**, 175302.
15 J. Cervera, B. Schiedt, R. Neumann, S. Mafe and P. Ramirez, *J. Chem. Phys.*, 2006, **124**, 104706.
16 Z. S. Siwy, *Adv. Funct. Mater.*, 2006, **16**, 735.
17 L. X. Zhang, S. L. Cai, Y. B. Zheng, X. H. Cao and Y. Q. Li, *Adv. Funct. Mater.*, 2011, **21**, 2103.
18 D. Momotenko, F. Cortes-Salazar, J. Josserand, S. J. Liu, Y. H. Shao and H. H. Girault, *Phys. Chem. Chem. Phys.*, 2011, **13**, 5430.
19 P.Yu.Apel., Yu.E.Korchev, Z.Siwy, R.Spohr and M.Yoshida, *Nucl. Instrum. Methods Phys. Res. B*, 2001, **184**, 10.
20 P. Y. Apel, I. V. Blonskaya, O. L. Orelovitch, B. A. Sartowska and R. Spohr, *Nanotechnology*, 2012, **23**, 225503.

21 P. Y. Apel, P. Ramirez, I. V. Blonskaya, O. L. Orelovitch and B. A. Sartowska, *Phys. Chem. Chem. Phys.*, 2014, **16**, 15214.
22 H. Zhang, X. Hou, Z. Yang, D. Yan, L. Li, Y. Tian, H. Wang and L. Jiang, *Small*, 2014, DOI: 10.1002/smll.201401677.
23 L. G. Molokanova, A. N. Nechaev and P. Y. Apel, *Colloid J.*, 2014, **76**, 170.
24 P. Ramirez, P. Y. Apel, J. Cervera and S. Mafe, *Nanotechnology*, 2008, **19**, 315707.
25 H. Zhang, X. Hou, L. Zeng, F. Yang, L. Li, D. Yan, Y. Tian and L. Jiang, *J. Am. Chem. Soc.*, 2013, **135**, 16102.
26 H. Zhang, Y. Tian and L. Jiang, *Chem. Commun.*, 2013, **49**, 10048.
27 S. Nasir, M. Ali, P. Ramirez, V. Gómez, B. Oschmann, F. Muench, M. Nawaz Tahir, R. Zentel, S. Mafe and W. Ensinger, *ACS Appl. Mater. Inter.*, 2014, **6**, 12486.
28 X. Hou, F. Yang, L. Li, Y. Song, L. Jiang and D. Zhu, *J. Am. Chem. Soc.*, 2010, **132**, 11736.
29 G. Nguyen, I. Vlassiouk and Z. S. Siwy, *Nanotechnology*, 2010, **21**, 265301.
30 B. Yameen, M. Ali, R. Neumann, W. Ensinger, W. Knoll and O. Azzaroni, *Nano Lett.*, 2009, **9**, 2788.
31 M. R. Powell, L. Cleary, M. Davenport, K. J. Shea and Z. S. Siwy, *Nat. Nanotechnol.*, 2011, **6**, 798.
32 M. Pevarnik, K. Healy, M. Davenport, J. Yen and Z. S. Siwy, *Analyst*, 2012, **137**, 2944.
33 Q. Chen, L. Meng, Q. Li, D. Wang, W. Guo, Z. Shuai and L. Jiang, *Small*, 2011, **7**, 2225.
34 J. Gao, W. Guo, D. Feng, H. Wang, D. Zhao and L. Jiang, *J. Am. Chem. Soc.*, 2014, **136**, 12265.
35 J. Zhang, Y. Yang, Z. Zhang, P. Wang and X. Wang, *Adv. Mater.*, 2014, **26**, 1071.
36 Q. Zhang, Z. Hu, Z. Liu, J. Zhai and L. Jiang, *Adv. Funct. Mater.*, 2014, **24**, 424.
37 O. Ayyad, D. Muñoz-Rojas, N. Agulló, S. Borrós and P. Gómez-Romero, *Soft Matter*, 2010, **6**, 2389.
38 B. Balakrishnan, M. Mohanty, P. R. Umashankar and A. Jayakrishnan, *Biomaterials*, 2005, **26**, 6335.
39 X. Yao, Z. Chen and G. Chen, *Electrophoresis*, 2009, **30**, 4225.
40 Y. Guo, X. Li and Y. Fang, *Electrophoresis*, 1998, **19**, 1311.
41 T. Lengyel and A. Guttman, *J. Chromatogr. A*, 1999, **853**, 511.
42 J. Liu, L. Chen, L.Lia, X.Hu and Y.Cai, *Int. J. Pharm.*, 2004, **287**, 13.
43 S. Matsukawa, Y. Ding, Q. Zhao, A. Mogi, Y. Tashiro and H. Ogawa, *Carbohydr. Polym.*, 2014, **109**, 166.
44 F. Xia, W. Guo, Y. Mao, X. Hou, J. Xue, H. Xia, L. Wang, Y. Song, H. Ji, Q. Ouyang, Y. Wang and L. Jiang, *J. Am. Chem. Soc.* , 2008, **130**, 8345.
45 Z. Siwy, P. Apel, D. Baur, D. D. Dobrev, Y. E. Korchev, R. Neumann, R. Spohr, C. Trautmann and K.-O. Voss, *Surf. Sci.*, 2003, **532–535**, 1061.
46 Z. Siwy and A. Fulinski, *Phys. Rev. Lett.*, 2002, **89**, 198103.
47 D. Woermann, *Phys. Chem. Chem. Phys.*, 2004, **6**, 3130.
48 H. Daiguji, Y. Oka and K. Shirono, *Nano Lett.*, 2005, **5**, 2274.
49 I. Vlassiouk, S. Smirnov and Z. Siwy, *ACS Nano*, 2008, **2**, 1589.
50 I. Vlassiouk, T. R. Kozel and Z. S. Siwy, *J. Am. Chem. Soc.*, 2009, **131**, 8211.